ECHO–HOLOGRAPHY IN DEGENERATE AND MULTILEVEL SYSTEMS

L.A. Nefed'ev and V.V. Samartsev

State Pedagogical Institute
and Physicotechnical Institute of the Russian Academy of Sciences, Kazan'
Received March 18, 1993

Some salient features are studied of optical transient processes such as photon echoes and their use in dynamic holography of degenerate and multilevel quantum systems. Applications are discussed of echo–holography to echo–spectroscopy, system of real–time data processing, and transformation of spatio–temporal structure of laser pulses.

By now a new promising line of investigation has been formed in holography, namely, dynamic holography (see review in Ref. 1 and the references to original studies cited therein). The structure of dynamic holograms is a function of not only the spatial coordinates of an object but also of time, while the process of dynamic holography by itself is considered as scattering of a probing beam by quasiperiodic inhomogeneities of a medium initiated by recording waves (in the case of high beam power these inhomogeneities are initiated by probing wave as well).[2] Numerous and diverse materials are used as recording media in dynamic holography. Resonant media were first used as recording media by Gerretsen[3] and Boersch and Eichler.[4] These experiments and more recent studies[5–9] have outlined the scope of resonance dynamic holography. Both recording and readout of the dynamic holograms were then performed simultaneously. Later Phillion et al.[10] made an important step forward, namely, reconstructed the hologram at a delayed moment determined by the lifetime of an excited state. The authors of Refs. 11 and 12 (and those of more recent studies[13–15]) suggested to make another important step, namely, to separate the object and reference beams in time. Thus one more measurement was introduced into the process of recording the hologram. The new line of investigation of holography was named echo–holography. It is generally recognized now.

Resonance dynamic echo–holograms are recorded onto the superposition of atomic and molecular states using the transient processes of the type of photon echo (PE), forecasted by Kopvillem and Nagibarov in 1962–1963 (see Refs. 16 and 17). It should be noted that there are some qualitative differences between the transient phenomena in the optical range and those in the radio–frequency range. They are, first of all, quite short laser wavelengths as compared to the dimensions of the sample and second, degeneracy of the energy levels in a certain quantum number. That is why the PE is sensitive to the spatial structure of exciting pulses and allows one to use the resonant media to form spectrally selective holograms and nonstationary images.

During recording echo–holograms in resonant media dynamic lattices with nonequilibrium population and polarization are formed. The former is described by the diagonal components of the density matrix while the latter – by its off–diagonal components. Both external probing signals and echo–signals may be scattered by these lattices. In echo–holography this process is performed automatically at prescribed instants of time. Note also that such holograms may be recorded by the technique of the burnt–out dip.[18–19]

The authors of Refs. 20 and 21 were the first to study the salient features of the echo–hologram formation onto degenerate energy levels and to demonstrate that the polarization characteristics of the electric field of the object wave and the type of the resonant transition appear to be the controlling factors in forming, reconstructing, and transforming the echo–holograms. Thus, the effect of inversion of polarization of the echo–hologram response was first forecasted[20,22] and then experimentally observed in ruby.[23] The analysis of polarization characteristics of the reconstructed echo–holograms performed in these studies indicated that in the general case the polarization of the reconstructed echo–hologram response depends on the relative orientation of the fields of the object and standing waves as well as on the direction in which the response is observed. Meanwhile the response wavefront appears to be dependent on the type of the wavefront of every component of the electric field of the object pulse (these components differ in sense of their polarization), while the contribution of each component depends on the geometry of the experiment, so that the response wavefront may be specially changed by way of selecting the appropriate geometry. Similar results were obtained for stimulated echo–hologram as well.

The recording of echo–holograms onto multilevel systems is of particular interest, since frequency conversion of the reconstructed signals becomes possible. It was demonstrated in Refs. 24–29 that in multilevel systems, in which the inhomogeneous broadenings of various resonant transitions are correlated, the real–time scale of the echo–hologram response may be converted. In this case the echo–hologram recording of a fast process may be protracted in the hologram response, and *vice versa*, depending on the relation between the carrier frequencies of the object pulse and the response. Multilevel systems used for recording echo–holograms are capable of recording the information about the object at different frequencies. Thus it appears possible to develop color echo–holography.[30–31] Individual colors in the object pulse may be shifted in time relative to each other, and differ in polarization, wavefront, and temporal structure. The reference and reproducing pulses may have their Fourier–spectra different from the spectrum of the object pulse, which opens up additional opportunities for the transform (processing) of color information.

Thus the echo–holograms can be used in the systems of real–time signal processing (signal filtering), transformation of the spatiotemporal structure of laser pulses, and correction of the signal wavefronts and for the development of high–capacity random–access memory of optical computers as well as in echo–spectroscopy.

0235-6880/93/07 457-09 $02.00

Therefore, a solution of these problems is of significant practical interest.

1. TECHNIQUES FOR DESCRIPTION OF THE INTERACTION OF SHORT LASER PULSES OF COMPLEX SPATIOTEMPORAL STRUCTURE WITH RESONANCE PARTICLES

During recording the echo–hologram, information about the object may be embedded in the spatiotemporal structure of the object pulse and in its polarization. Two approaches are possible to the mathematical description of the interaction of that pulse with resonance particles. Neglecting relaxation within the time over which the pulse acts for a single–particle wave function ψ we have

$$i\hbar \frac{\partial}{\partial t}\psi = [\mathcal{H}_0 + V(\mathbf{r}, t)]\,\psi , \qquad (1)$$

where $V(\mathbf{r}, t)$ is the operator of interaction of the resonant particle with the exciting pulse and $\mathcal{H}_0$ is the unperturbed Hamiltonian. Proceeding to a rotating system of coordinates by the transformation

$$\tilde{\psi} = \exp(iAt)\,\psi , \qquad (2)$$

we obtain

$$\frac{\partial \tilde{\psi}}{\partial t} = -\frac{i}{\hbar}(B' + B'')\,\tilde{\psi} , \qquad (3)$$

where $B' = \tilde{\mathcal{H}}_0 - \hbar A$, $B'' = \tilde{V}(\mathbf{r}, t)$, $\tilde{\mathcal{H}}_0 = e^{iAt}\,\mathcal{H}_0\,e^{-iAt}$, and

$\tilde{V} = e^{iAt}\,V\,e^{-iAt}$.

Let us represent $\tilde{\psi}$ in the form

$$\tilde{\psi} = U\,\psi^{\circ} , \qquad (4)$$

where U is the operator of evolution. Then

$$\frac{\partial U}{\partial t} = -\frac{i}{\hbar}(B' + B'')\,U \qquad (5)$$

with the initial condition $U(0) = I$, where I is the unit matrix. The solution of this equation may be represented in the form $U = U_1(B')U_2(B'')$, where

$$\frac{\partial U_1}{\partial t} = -\frac{i}{\hbar}B'U_1 \qquad (6)$$

$$\frac{\partial U_2}{\partial t} = -\frac{i}{\hbar}U_1^{-1}B''U_1U_2 = Q\,U_2 . \qquad (7)$$

The solution of Eq. (6) has the form $U_1 = \exp\left(-\frac{i}{\hbar}B't\right)$, while the solution of Eq. (7) may be formally written as

$$U_2 = \mathrm{T}\exp\left\{-\frac{i}{\hbar}\int_{\Delta t} U_1^{-1}B''U_1\,dt\right\} =$$

$$= \sum_{n=0}^{\infty}\frac{1}{n!}\int_{\Delta t}dt_1\int_{\Delta t}dt_2 \ldots \int_{\Delta t}dt_n\,\mathrm{T}\,Q(t_1)\ldots\mathrm{T}\,Q(t_n) , \qquad (8)$$

where T is the Dyson operator.

In certain cases this series may be summed up to obtain an approximate solution of the problem. Note that matrix elements of the operator U_2 will then be expressed via the Fourier spectra of $V(t)$. Knowing the operator of evolution U we may define the density matrix upon exposure to the pulse

$$\rho = U\,\rho\,U^{-1} .$$

Knowing ρ we find the dipole moment $\mathbf{d} = \mathrm{Sp}(\rho\mathbf{d})$, and the strength of the electric field response in the wave zone

$$\mathbf{E} = \frac{1}{c^2}\sum_j \frac{1}{|\mathbf{R}_0 - \mathbf{r}_j|}\left(\langle\ddot{\mathbf{d}}_j(\mathbf{r}_j, \mathbf{n}_j, t')\rangle\times\mathbf{n}_j\right)\times\mathbf{n}_j , \qquad (9)$$

where $\mathbf{n}_j$ is the unit vector directed from the point $\mathbf{r}_j$ to the observation point $\mathbf{R}_0$,

$$t' = t - \frac{\mathbf{R}_0\,\mathbf{n}_j}{c} + \frac{\mathbf{r}_j\,\mathbf{n}_j}{c} .$$

A different approach based on the techniques of spectral analysis appears to be more convenient in certain cases.[32] It is applicable to relatively low intensity of exciting pulse in the absence of field broadening[33] and spectral diffusion within the time over which the pulse acts. The result of exposure of the object field to an atom may then be found by calculating the results of exposure of individual Fourier components of the pulse field to this atom with subsequent integration of these results over all virtual frequencies. Thus, if the field of the object pulse is given by

$$E = E_0\,\varepsilon(t)\cos(\omega t - \mathbf{kr}) , \qquad (10)$$

where $\varepsilon(t)$ describes the pulse shape, it may be represented as

$$E = \frac{E_0}{2}\left[\int_{-\infty}^{\infty}\tilde{\varepsilon}(\omega')\exp(i\,\omega' t + i\mathbf{kr} - i\,\omega\,t)\,d\omega' + \mathrm{c.c.}\right], \qquad (11)$$

where $\tilde{\varepsilon}(\omega') = \int_{-\infty}^{\infty}\varepsilon(t)\exp(-i\omega' t)\,dt$. That is, the problem of finding the density matrix in the given approximation is reduced to finding a solution for the Fourier component $\rho(\omega')$ when the atom is exposed to the radiation field

$$E(\omega') = E_0\,\tilde{\varepsilon}(\omega')\cos[(\omega - \omega')\,t - \mathbf{kr}] \qquad (12)$$

and to subsequent integrating $\rho(\omega')$ over all ω'.

Specific calculations by the above–described procedures indicate that the matrices of the operator of evolution, obtained by chronological ordering and spectral analysis, coincide for small pulse area and close to the resonance.

To describe the process of recording the echo–hologram, a certain approximation for recording of the object field and procedure for calculating the non–equilibrium polarization of the system must be chosen. In general, the electric field strength of the object wave will be (see Fig. 1)

$$\begin{aligned} E_x &= E_0\,\varepsilon_x(\mathbf{r}, t)\cos[\omega t - g_x(\mathbf{r}, t)] , \\ E_y &= E_0\,\varepsilon_y(\mathbf{r}, t)\cos[\omega t - g_y(\mathbf{r}, t)] , \\ E_z &= E_0\,\varepsilon_z(\mathbf{r}, t)\cos[\omega t - g_z(\mathbf{r}, t)] , \end{aligned} \qquad (13)$$

where E_0 is the field amplitude, ε is the parameter specifying the spatiotemporal inhomogeneity of the field, g_i = const defines the wavefront of the object wave, and ω is the cyclic carrier frequency.

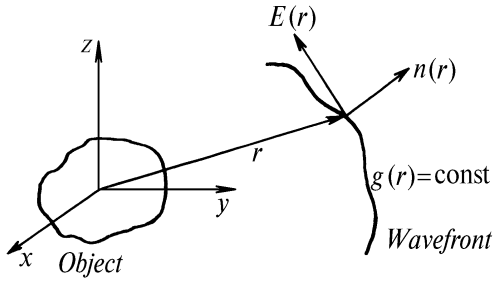

FIG. 1. Arbitrarily polarized object field as an illustration.

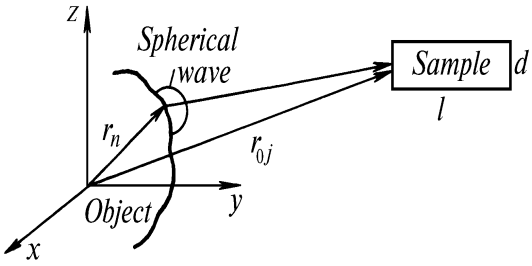

FIG. 2. Expansion of the object field into a series in spherical or plane waves as an illustration.

Prescribing the object wave in the form of Eq. (13) appears to be not always convenient for calculation of the field and interpretation of the results obtained. It sometimes appears handier to represent each Fourier component of the object wave as an expansion in spherical or plane waves (Fig. 2). In this case the object is considered as a set of points (denoted by the subscript n). Each point produces its own spherical wave. The combination of such waves at the point $\mathbf{r}_{0j}$ yields perturbation at the site of a working particle in the sample. Mathematically the electric field strength at the point $\mathbf{r}_{0j}$ may be written as

$$E = \sum_n A_{nj} \frac{\exp(i\,\mathbf{k}_n(\mathbf{r}_{0j} - \mathbf{r}_n) - i\,\omega\,t + i\,\mathrm{j}_n)}{|\mathbf{r}_{0j} - \rho_n|} = \sum_n A'_{nj} \frac{\exp(i\,\mathbf{k}_n(\mathbf{r}_{0j} - \mathbf{r}_n) - i\,\omega\,t)}{|\mathbf{r}_{0j} - \mathbf{r}_n|}, \qquad (14)$$

where $\mathbf{k}_n = \frac{\omega}{c}\mathbf{n}_n$, $\mathbf{n}_n = \frac{\mathbf{r}_{0j} - \mathbf{r}_n}{|\mathbf{r}_{0j} - \mathbf{r}_n|}$, and φ_n describes the initial phases of spherical waves, moreover, the term $\exp(i\varphi_{nj})$ may be introduced into the complex amplitudes A_{nj} (the subscript j implies that A depends on the orientation of $\mathbf{n}_n$ in the general case). When the dimensions of the object are small as compared to the distance to it, i.e., $|\mathbf{r}_{0j} - \mathbf{r}_n| \gg d$, l and $|\mathbf{r}_{0j} - \mathbf{r}_n| \gg |\mathbf{r}_n|$, the expansion in the spherical waves transforms into the expansion in the plane waves

$$E = \sum_n a'_n \, \mathrm{e}^{\,i\,\mathbf{k}_n\,\mathbf{r}_{0j} - i\,\omega\,t}. \qquad (15)$$

The form of this expansion is similar to the spatial Fourier transform in the plane waves, but the physical meaning of the coefficients a'_n is that they define the amplitudes of the field (amplitudes of the Fourier components of the field) coming from individual points of the object.

Since in this approximation the dimensions of the resonant medium are considered to be much smaller than the distance to the object, perturbation at each point of the sample is then produced by practically one and the same combination of the plane waves.

2. FORMATION OF ECHO–HOLOGRAMS AT DEGENERATE LEVELS

Let us consider the effect of polarization of electric field of object wave pulse and of the structure of the resonant transition on the formation and reconstruction of echo–holograms. As demonstrated below, these are the characteristics of polarization of the electric field of the object wave and the type of the resonant transition, which appear to be decisive in certain cases of forming, reconstructing, and transforming such holograms. For our model we choose the transition on which the total moment change is 1/2–1/2 and consider the formation of echo–holograms during the recording of the object field with arbitrary phase front, polarization, temporal structure, and spatial orientation. We specify the field strength of the first pulse of the object wave in the form of Eq. (13) and consider the formation of the reconstructed echo–hologram. In this case we take the pulse of the standing wave aribitrarily oriented in space for the second pulse. To this end we set $g_i = 0$ $(i = x', y', z')$, $\varepsilon_{z'} = \cos \mathbf{k}_2\mathbf{r}$, and $\varepsilon_{x'} = \varepsilon_{y'} = 0$ in Eq. (13), where $\mathbf{k}_2$ is the wave vector of the running waves which form the standing wave. The vector of the electric field strength of the standing wave is assumed to be oriented along the z' axis of the coordinate system (x', y', z') being arbitrarily oriented with respect to the laboratory system of coordinates (x, y, z) used to specify the field of the object wave. The orientation of the coordinate system (x', y', z') with respect to (x, y, z) will be determined by the Euler angles α_{12}, β_{12}, and γ_{12}. In calculating the density matrix of the system after exposure to the pulses of the object and standing waves, account must be taken of the fact that each individual atom appears to be optically oriented after exposure to the pulse of the object wave; therefore, the solution for the density matrix of the system can be constructed in the (x, y, z) coordinate system.

If the standing wave of the second pulse is arbitrarily oriented in space, the matrix of the operator of interaction with the second pulse, in the (x, y, z) system of coordinates, can be written in the form

$$\langle J_1 M_1 | V | J_2 M_2 \rangle = \sum_{MK} D^{J_1}_{KM_1} D^{J_2}_{KM_2} V_{J_1 K J_2 M}, \qquad (16)$$

where $V_{J_1 K J_2 M}$ is the matrix element of the operator of interaction in the (x', y', z') system of coordinates and $D^J_{MM'}$ are the Wigner functions, which specify the conversion between the systems of coordinates for the first and the second pulses. The virtual transitions and the spectrum of excitation for the reconstructed echo–hologram are shown in Fig. 3.

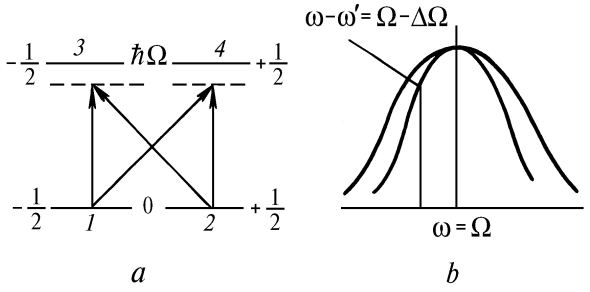

FIG. 3. Formation of echo–holograms onto degenerate energy levels. a) Scheme of energy transitions excited during recording of the echo–holograms, b) spectrum of excitation: ΔΩ is the spread of frequencies (inhomogeneous broadening) and ω′ are the frequencies of the Fourier spectrum of the object wave pulse.

To obtain an adequate polarization of the echo–hologram response given by Eq. (9), the components of the vector **d** must be specified in the right–handed system of coordinates irrespective of the direction of observation. Thus it appears convenient to introduce a mobile system of coordinates (x_1, y_1, z_1), affixed to that direction with the z_1 axis, for example, along the direction of response **n**, and to convert the components of the vector **d** to this system of coordinates [with the use of the rotation matrix $A(\alpha, \beta, \gamma)$].

The angular dependence of the electric field strength in the response of the reconstructed echo–hologram was found in Ref. 20 in the case in which the pulse spectrum was narrower than the spectrum of the inhomogeneously broadened line

$$\mathbf{E} \sim \sum_j \int_{-\infty}^{\infty} d\omega' f_{2j} f_{4j} \frac{a_{2j}^{*2}}{|a_2|^2} \sin^2\theta_{2j} \times$$

$$\times \{[(\cos\alpha \cos\beta \cos\gamma - \sin\alpha \sin\gamma) F_1 +$$

$$+ (\cos\alpha \cos\beta \sin\gamma + \sin\alpha \cos\gamma) F_2 + \cos\alpha \sin\beta F_3] \mathbf{i}_1 +$$

$$+ [(\sin\alpha \cos\beta \cos\gamma + \cos\alpha \sin\gamma) F_1 -$$

$$- (-\sin\alpha \cos\beta \sin\gamma + \cos\alpha \cos\gamma) F_2 + \sin\alpha \sin\beta F_3] \mathbf{j}_1\} \times$$

$$\times \exp(2\tau/T_2) \exp[-i(\Omega + \omega')(t' - 2\tau)] + \text{c.c.}\,, \qquad (17)$$

where a_2 is the matrix element of the operator of interaction with the standing wave pulse, θ_2 is the standing wave pulse area, $\mathbf{i}_1$ and $\mathbf{j}_1$ are the unit vectors of the coordinate system (x_1, y_1, z_1) affixed to the direction of response, τ is the time interval between the pulses of the object and standing waves, T_2 is the rate of the irreversible transverse relaxation,

$$F_1 = \tilde{\varepsilon}_z e^{-i\tilde{g}_z} \sin 2\beta_{12} \cos\gamma_{12} - \tilde{\varepsilon}_x e^{-i\tilde{g}_x} \times$$

$$\times (\sin^2\beta_{12} \cos 2\gamma_{12} - \cos^2\beta_{12}) - \tilde{\varepsilon}_y e^{-i\tilde{g}_y} \sin^2\beta_{12} \sin 2\gamma_{12}\,,$$

$$F_2 = \tilde{\varepsilon}_z e^{-i\tilde{g}_z} \sin 2\beta_{12} \sin\gamma_{12} - \tilde{\varepsilon}_x e^{-i\tilde{g}_x} \times$$

$$\times \sin^2\beta_{12} \sin 2\gamma_{12} + \tilde{\varepsilon}_y e^{-i\tilde{g}_y} (\sin^2\beta_{12} \cos 2\gamma_{12} + \cos^2\beta_{12})\,,$$

$$F_3 = -\tilde{\varepsilon}_z e^{-i\tilde{g}_z} \cos 2\beta_{12} + \tilde{\varepsilon}_x e^{-i\tilde{g}_x} \sin 2\beta_{12} \cos\gamma_{12} +$$

$$+ \tilde{\varepsilon}_y e^{-i\tilde{g}_y} \sin 2\beta_{12} \sin\gamma_{12}\,,$$

$\tilde{\varepsilon}_i \exp(-i\tilde{g}_i)$ is the Fourier spectrum of the object wave pulse envelope,

$$f_2 = \frac{1}{2} (\cos\theta_1 \sqrt{\varphi + \varphi'} + \cos\theta_1 \sqrt{\varphi - \varphi'})\,,$$

$$f_4 = (\sqrt{\varphi + \varphi'})^{-1} \sin\theta_1 \sqrt{\varphi + \varphi'} + (\sqrt{\varphi - \varphi'})^{-1} \sin\theta_1 \sqrt{\varphi - \varphi'}\,;$$

$$\theta_1 = \hbar^{-1} E_0 \, d\Delta \, t_1\,, \quad \varphi = \frac{1}{6} \sum_i \tilde{\varepsilon}_i\,,$$

$$\varphi' = \frac{1}{3} [\tilde{\varepsilon}_z^2 \tilde{\varepsilon}_x^2 \sin^2(\tilde{g}_x - \tilde{g}_z) + \tilde{\varepsilon}_z^2 \tilde{\varepsilon}_y^2 \sin^2(\tilde{g}_y - \tilde{g}_z) +$$

$$+ \tilde{\varepsilon}_x^2 \tilde{\varepsilon}_y^2 \sin^2(\tilde{g}_y - \tilde{g}_x)]^{1/2}\,.$$

Analysis of Eq. (17) shows that the polarization of the reconstructed echo–hologram response depends in the general case on the direction of observation as well as on the orientation of the standing wave field. Therefore, the polarization of response can be inverted by varying the angles β_{12} and γ_{12}, which determine the orientation of the electric field of the standing wave. And because in the general case the polarization of the object wave field is different in different parts of the sample, we may obtain differently polarized responses by scanning the standing wave across the volume of the sample. That is, when the information about the object is embedded in the polarization of the object wave pulse, it can be read. The wavefront phase of the reconstructed echo–hologram response turns out to be dependent on the wavefront phases of all the components of electric field of the object wave (coefficients F_i). Moreover, the contribution of each component to the response wavefront appears to be dependent on the direction of observation and on the relative orientation of the fields of the object and standing waves. Thus directional change (i.e., transformation) of the response wavefront is possible by varying the corresponding Euler angles.

The factor

$$f_2 f_4 \sin^2\theta_2 \qquad (18)$$

in expression (17) depends on the spatiotemporal structure of the object wave field, which may result in nonlinear reproduction of the echo–hologram. By expanding expression (18) into a series in the Bessel functions J and the Chebyshev polynomials T we find

$$\sin^2\theta_2 f_2 f_4 = \frac{1}{4} \left[1 - J_0(2\theta_2)) - 2 \sum_{n=1}^{\infty} J_{2n}(2\theta_2) \cos(2n\mathbf{k}_2\mathbf{r}_j)\right] \times$$

$$\times \sum_{n'=0}^{\infty} (-1)^{n'} \left[J_{2n'+1}(2\theta_1)\left(\frac{1}{x} T_{2n'+1}(x) + \frac{1}{x'} T_{2n'+1}(x')\right) +\right.$$

$$\left. + J_{2n'+1}(\theta_1) T_{2n'+1}(x + x') \left(\frac{1}{x} + \frac{1}{x'}\right)\right], \qquad (19)$$

where $x = \sqrt{\varphi + \varphi'}$ and $x' = \sqrt{\varphi - \varphi'}$.

That is, the complex dependence of the factor given by Eq. (18) on the spatiotemporal structure of the field of the object wave appears to be separated in Eq. (19) in the Chebyshev polynomials. Therefore, it follows from expression (19) that linear reproduction of the echo–hologram is possible only if a major contribution to its

response comes from the term of the expansion containing $J_1(2\theta_1)$. In this case $T_1(x) = x$ and $f_2 f_4 = J_1(2\theta_1)$. As the electric field strength of the object wave pulse increases, other terms of expansion (19) start to make a contribution to the response of the echo–hologram, resulting in its nonlinear reproduction. Thus the limiting condition $\theta_1 < 1$ is imposed on the object pulse area.

Note also that F_1, F_2, and F_3 depend in the general case on all the quantities ε_i and g_i resulting in a shift and transformation of the spatiotemporal structure of the response to each component of the electric field of object wave, so that the efficiency of such transformations depends on the relative orientation of exciting fields.

Now we consider two important cases in which the object wave has close–to–linear or elliptic (circular) polarization.

In the first case with arbitrary orientation of the polarization vectors of electric fields of object and standing waves the polarization of response will be elliptic. If the polarization vectors of object and standing waves are parallel, that is, $\alpha_{12} = \beta_{12} = \gamma_{12} = 0$, we have $F_1 = F_2 = 0$, $F_3 = -\tilde{\varepsilon}_{zz} e^{-i\tilde{g}_z}$, and

$$\mathbf{E} \sim \sum_i \int_{-\infty}^{\infty} d\omega' J_1(2\theta_1)(1 - J_0(2\theta_1))\Big[-\cos\alpha \sin\beta\, \tilde{\varepsilon}_z \exp(-i\tilde{g}_z)\, \mathbf{i}_1 -$$

$$- \sin\alpha \sin\beta\, \tilde{\varepsilon}_z \exp(-i\tilde{g}_z)\, \mathbf{j}_1\Big] \exp\left(-\frac{2\tau}{T_2}\right) \times$$

$$\times \exp[-i(\Omega + \omega')(t' - 2\tau)] + \text{c.c.} \qquad (20)$$

If we represent $\tilde{\varepsilon}_z e^{-i\tilde{g}_z}$ as an expansion in the plane waves

$$\tilde{\varepsilon}_z \exp(-i\tilde{g}_z) = \sum_n \varepsilon_n \exp\left(-i\mathbf{n}_n \mathbf{r}\, \frac{\omega - \omega'}{c}\right), \qquad (21)$$

then the following conditions of spatial wave synchronization will be satisfied for individual spatial components of the electric field of the echo–hologram response:

$$\mathbf{n}_{en} = \mathbf{n}_n .$$

Thus the wavefront of the response appears to be phase conjugate so that conditions of observations for each component of the response will be $\alpha = 90°$, $\beta = 270°$, and $\gamma = 270°$.

For $T_2^* \ll \Delta t$ integration over ω' in Eq. (20) yields the shape of the response

$$\langle \exp(-i\omega'(t - 2\tau)\, \tilde{\varepsilon}_z \exp(-i\tilde{g}_z) \rangle_{\omega'} , \qquad (22)$$

which is the inverse Fourier–transform of the complex conjugate value of $\tilde{\varepsilon}_z \exp(-i\tilde{g}_z)$. Therefore, the waveform of the response in this particular case is reversed in time to that sequence of events the information about which is embedded in the object wave (see Fig. 4). In Ref. 34 ruby was used to test experimentally the phase conjugation (of spherical wave) and reversed waveform of the echo–hologram response for linearly polarized exciting pulses. Block diagram of the setup used to test the phase conjugation of the echo–hologram in the ruby crystal [onto the transition $^4A_2 - {}^2E(E)$] is shown in Fig. 5*a*. The sample S is upon exposure to the two pulses of the running and standing waves. The radiation of the first pulse is focused with the lens L of focal distance R onto the sample S. The second pulse, delayed by the optical delay line (ODL), is fed into the same sample as a plane wave. The standing wave is formed using a mirror. The reconstructed echo–hologram signal is fixed in the direction opposite to that of the first pulse by means of the semitransparent mirror STM_2. The divergence of this beam and hence the curvature radius of its wavefront may be found from the diameter of the diaphragm d_2. An increase of the diameter d_2 to d_1 corresponded to a rise in the response intensity (if the distance d_2–$STM_2 - S$ (was equal to SL). Further increase of the diameter of the diaphragm ($d_2 > d_1$) did not produce a noticeable rise in the signal intensity. This meant that the divergence of the echo–signal beam was equal to the angle of convergence of the object wave beam, which corresponded to a situation when the wavefront of the reconstructed echo–hologram response was phase–conjugate to the wavefront of the running wave. Figure 5*b* shows the waveform of the reconstructed echo–hologram response, in which one can observe the reversed waveform of the response to that of the object wave.

Now we consider the second limiting case in which the polarization of the electric field of the object wave is close to elliptic. In this case the observing conditions for the individual spatial components of the echo–hologram response will be $\alpha = \gamma = 0$ and $\beta = 180°$, while F_i will be given by the formulas

$$F_1 = -\tilde{\varepsilon}_x e^{-i\tilde{g}_x} (\sin^2\beta_{12} \cos 2\gamma_{12} - \cos^2\beta_{12}) -$$

$$- \tilde{\varepsilon}_y e^{-i\tilde{g}_y} \sin^2\beta_{12} \sin 2\gamma_{12} ,$$

$$F_2 = -\tilde{\varepsilon}_x e^{-i\tilde{g}_x} \sin^2\beta_{12} \sin 2\gamma_{12} +$$

$$+ \tilde{\varepsilon}_y e^{-i\tilde{g}_y} (\sin^2\beta_{12} \cos 2\gamma_{12} + \cos^2\beta_{12}) . \qquad (23)$$

It follows from Eq. (23) that γ_{12} remains equal to zero when the orientation of the vector of the electric field strength of the standing wave changes only in the plane in which the wave vector $\mathbf{k}_2$ lies. When the angle β_{12} changes from 0 to 90° (that is, the polarization vector of the standing wave changes its direction), the polarization of the response converts from counterclockwise at $\beta_{12} = 0°$ to clockwise at $\beta_{12} = 90°$ (for counterclockwise polarization of the object pulse). The effect of inversion of polarization of the echo–hologram response was predicted in Refs. 20–22 and experimentally observed in Ref. 23. The experimental setup is shown in Fig. 6.

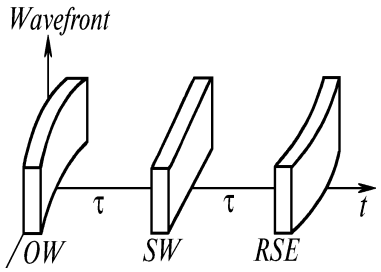

FIG. 4. Phase conjugation and reversion of the echo–hologram form in case of linearly polarized pulses as an illustration.

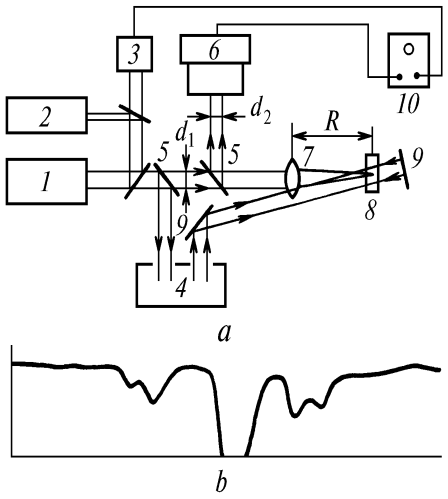

FIG. 5. Reconstructed echo–holograms in ruby (after Ref. 34). a) Block diagram of the experimental setup: 1) low–temperature ruby laser, 2) tuning laser, 3) synchronous photodetector, 4) optical delay line (ODL), 5) semitransparent mirrors (STM's), 6) recording photodetector, 7) spherical lens of focal distance R, 8) examined ruby crystal, 9) mirrors, and 10) period meter. Here d_1 and d_2 are diaphragms. b) RSE (reversed signal of exho–hologram waveform).

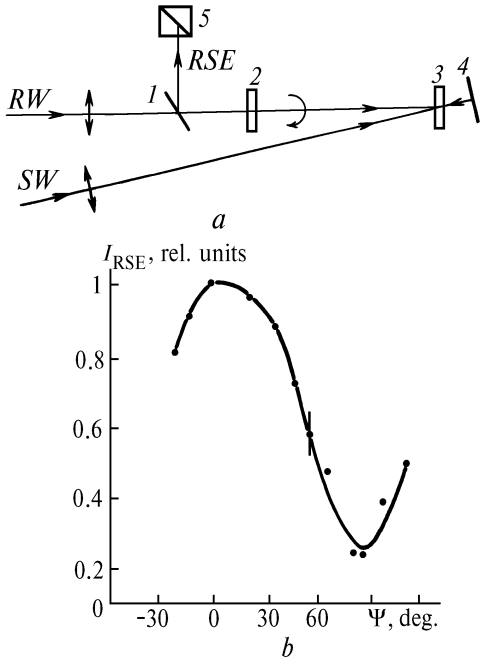

FIG. 6. The effect of inversion of photon echo–polarization in ruby (from Ref. 23). a) Scheme of excitation of the reconstructed photon echo by the circularly polarized running wave (RW) pulse and linearly polarized standing wave (SW) pulse: 1) semitransparent mirror, 2) quarter–wave plate, 3) examined ruby crystal, 4) mirror forming the standing wave, and 5) analyzer. b) The dependence of the intensity of echo–signal I_{RSE} on the angle of rotation of the analyzer.

To excite the RSE by the circularly polarized radiation, the quarter–wave plate *2* was placed in the beam of running object wave (RW). Sense of linear polarization of the response at the exit from the quarter–wave plate is determined by the sense of circular polarization of the RSE. If the circular polarization of the response and that of the RW have one sense, the response at the exit from the quarter–wave plate will be linearly polarized and the sense of its polarization will be perpendicular to that of the linear polarization of the RW. This situation is similar to the rotation of the plane of polarization by 90° due to the double passage of the quarter–wave plate. If the sense of circular polarization of the response is opposite to that of the RW after it passes through the quarter–wave plate, then the response will be linearly polarized due to the passage of the quarter–wave plate and will have one sense of polarization with the initial linear polarization of the RW. In the same way, using ruby as an example, we were able to find that if the RSE was excited by a pulse of the circularly polarized running wave and a pulse of the linearly polarized standing wave (SW) ($\gamma_{12} = 0$ and $\beta_{12} = 90°$), the response would be circularly polarized in the direction counter to that of polarization of the RW. This result is testified by the dependence of the RSE intensity on the angle between its sense of polarization and the sense of initial polarization of the RW shown in Fig. 6 *b*.

Stimulated echo–holograms recorded onto degenerate levels have similar properties. Thus a limitation is imposed on the object pulse area (of the first or second pulse), which follows from an expansion similar to expression (20) (see Ref. 21). Linear reproduction of the stimulated echo–hologram is feasible only when $\theta \approx 1$. As the electric field strength of the object wave increases, the dependence of the electric field strength of the response on the spatiotemporal structure of the object wave field becomes nonlinear. Such a behavior of the echo–hologram response was experimentally observed in Ref. 35, where all the pulses were linearly polarized and the second was the code (object) pulse.

Theoretical analysis performed in Ref. 21 revealed that when all three pulses are identically linearly polarized and the spectral width of the object wave pulse is narrower than the width of the inhomogeneously broadened transition line, the object pulse waveform may be reproduced with minimum distortions. Moreover, if the first pulse is the object one, the spatiotemporal structure of the field of the echo–hologram response will be conjugate to that of the object wave. Now, if the object pulse is second, the reproduced echo–hologram will reconstruct the spatiotemporal structure of the object wave field (Fig. 7).

The last case was experimentally studied in Ref. 35, and Fig. 8 shows waveforms illustrating the correlation between the shapes of the echo–hologram response and object pulse.

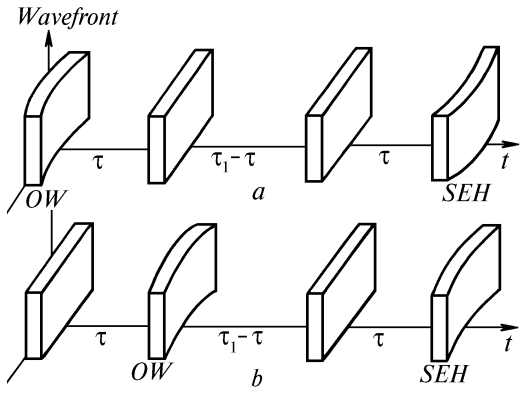

FIG. 7. The process of formation of stimulated echo–holograms by the linearly polarized pulses as an illustration. a) Object pulse is first and b) object pulse is second.

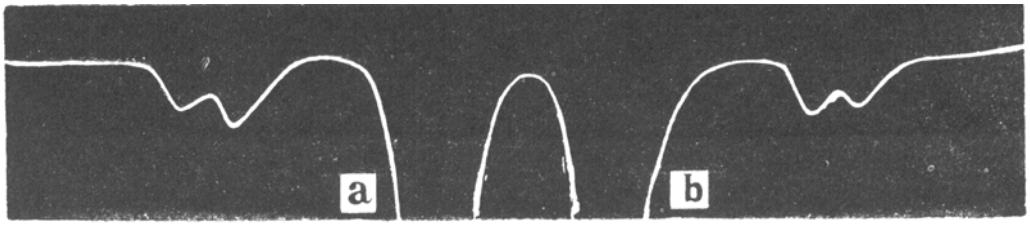

FIG. 8. The effect of correlation between the waveforms of stimulated photon echo in ruby[35]: a) object pulse and b) echo–pulse.

Recording and reconstructing the stimulated echo–holograms (SEH) make it possible to compare (identify) the phase structure of the object field.[21] This is done by recording the object pulse and adding the reference pulse (pulses) of known phase front. That third pulse has a flat wave front. In this case the electric field strength of the echo–hologram response peaks at $\tilde{g}_z^{(2)} = \tilde{g}_z^{(1)}$, that is, when the phase fronts of the object and reference pulses are identical. The orientation of the vector $\mathbf{k}_3$ may then be arbitrary, and the wavefront of the response may be plane. Meanwhile, if $\tilde{g}_z^{(2)} \neq \tilde{g}_z^{(1)}$, the spatial phase synchronization is either completely disrupted or occurred only for a limited number of spatial components of the electric field strength of the object and reference waves, resulting in a decrease in the integral intensity of the response. That is, it is experimentally feasible to use a set of prescribed reference fields with known wavefronts to identify the front of the object pulse (to recognize its image) observing the integral intensity of the stimulated echo–hologram response.

3. MULTIFREQUENCY ECHO–HOLOGRAPHY

Recording and reconstructing the echo–holograms onto multilevel systems is of particular interest when the frequency conversion of the reconstructed signals is feasible[30,31] since information about the object can be recorded at different frequencies using object pulses with several carrier frequencies analogous to color holography in non–resonant media.[1]

Information about the color of the object in the echo–hologram is apparently embedded in a set of lattices with non–equilibrium population (polarization) of different energy levels of the multilevel system. Figure 9 illustrates a possible scheme of recording the echo–hologram onto a four–level system, the three carrier frequencies in which play the role of colors (note that in principle echo–holography permits one to use any number of frequencies, provided the corresponding transitions present in the sample). The first or second pulse may be the object pulse. Color echo–holography may be used in systems of multichannel data processing and storage.

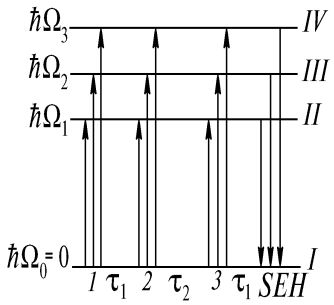

FIG. 9. Formation of color echo–holograms in the system sharing a common energy level.

Now we consider the process of formation of the stimulated color echo–hologram (Fig. 9). In this case the electric field strength of the ηth pulse is written as

$$E_\eta = \sum_{i=1}^{3} E_{0i}^{(\eta)} \varepsilon_i^{(\eta)}(\mathbf{r}, t) \cos\left(\omega_i t - g_i^{(\eta)}(\mathbf{r}, t)\right), \qquad (24)$$

where ω_i is the carrier frequency, E_{0i} is the amplitude of the electric field strength, g_i is the wavefront, and $\varepsilon_i^{(\eta)}$ is the parameter describing the spatiotemporal inhomogeneity of the field. In this particular case the Fourier–analysis is inapplicable in calculating the operator of evolution of the system. Therefore, it is necessary to use the technique of chronologic ordering outlined in Sec. 1. The Hamiltonian of the system may be represented in the form

$$\mathcal{H}_0 = \hbar\,\Omega_1 \begin{pmatrix} 0 & 0 & 0 & 0 \\ 0 & 1 & 0 & 0 \\ 0 & 0 & \Gamma_1 & 0 \\ 0 & 0 & 0 & \Gamma_2 \end{pmatrix}, \qquad \begin{aligned} \Omega_1 \Gamma_1 &= \Omega_2, \\ \Omega_1 \Gamma_2 &= \Omega_3, \end{aligned} \qquad (25)$$

where the quantities Γ_i characterize the non–equidistant system spectrum. The Hamiltonian of interaction of the jth particle with local fields may then be written in the form

$$\mathcal{H}_{\text{in}}^{j} = \hbar\,\Delta\Omega_1^{j} \begin{pmatrix} 0 & 0 & 0 & 0 \\ 0 & 1 & 0 & 0 \\ 0 & 0 & \Gamma_1 m_1 & 0 \\ 0 & 0 & 0 & \Gamma_2 m_2 \end{pmatrix}, \qquad (26)$$

where $\Delta\Omega_1$ is the deviation of the frequency of the 1–2 transition from its statistical mean and m_i defines dissimilarity of the interaction between the optical electron in its different states and the local field.

Taking into account all the above we obtain for the spatiotemporal structure of the field of the echo–hologram response (e.g., on the 1–2 transition)[31]

$$E \sim \sum_{j\,n} B_1 A_1^{(3)} \tilde{S}_1^{(3)} \sin\frac{2\theta_1}{\hbar} \sin\frac{2\theta_3}{\hbar} \left\{ A_1^{(1)*} A_1^{(2)} \tilde{S}_1 \times \right.$$

$$\left. \times \int_{-\infty}^{\infty} d\Delta\Omega_1 \tilde{S}_1^{(2)}(\Delta\Omega_1) \exp\left\{ i\Delta\Omega_1 (t_e - t_1 - 2\tau) - \frac{2\tau}{\tau_{12}} + i\mathbf{k}_{ep}(\mathbf{r}_j - \mathbf{R}_0) \right\} + \right.$$

$$+ A_2^{(1)*} A_2^{(2)} \tilde{S}_2^{(1)*} \int_{-\infty}^{\infty} d\Delta\Omega_1 \tilde{S}_2^{(2)}(\Gamma_1 m_1 \Delta\Omega_1) \times$$

$$\times \exp\left\{ i\Delta\Omega_1 (t_e - \tau_1 - \tau) - i\,\Gamma_1 m_1 \Delta\Omega_1 \tau - \frac{\tau}{\tau_{12}} - \frac{\tau}{\tau_{31}} + \mathbf{k}_{ep}\,\mathbf{r}_j \right\} +$$

$$+ A_3^{(1)*} A_3^{(2)} \tilde{S}_3^{(1)*} \int_{-\infty}^{\infty} d\Delta\Omega_1 \tilde{S}_3^{(2)}(\Gamma_2 m_2 \Delta\Omega_1) \times$$

$$\times \exp\left\{ i\Delta\Omega_1 (t_e - \tau_1 - \tau) - i\Gamma_2 m_2 \Delta\Omega_1 \tau - \frac{\tau}{\tau_{12}} - \frac{\tau}{\tau_{41}} + \mathbf{k}_{ep} \mathbf{r}_j \right\} \Big\} \quad (27)$$

where $S_i^{(\eta)} = \varepsilon_i^{(\eta)} \exp(-i g_i)$, $A_i^{(\eta)} = d_{1i} \frac{E_{0i}^{(\eta)}}{2}$,

$$\tilde{S}_i = \int_{t_\eta - \frac{\Delta t_\eta}{2}}^{t_\eta + \frac{\Delta t_\eta}{2}} S_i \exp\left(-i \frac{\Delta_i}{\hbar} t \right) d\, t,$$

τ_{ij} are the relaxation coefficients for the off–diagonal elements of the density matrix, $\mathbf{k}_{ep}$ are the wave vectors of the plane waves from the spatial expansion of the response field. Each integral in expression (27) is the inverse Fourier transform of the corresponding spectrum $\tilde{S}_i^{(2)}$ (object pulse). By expanding $S_i^{(2)}$ into a series in the plane waves with the vectors $\mathbf{k}_{ip}^{(2)}$, we obtain from Eq. (27) the conditions of phase synchronization for the response of the color echo–hologram

$$\mathbf{k}_{ep} + \mathbf{k}_i^{(1)} - \mathbf{k}_{ip}^{(2)} - \mathbf{k}_i^{(3)} = 0 \quad (28)$$

and the moments at which responses are produced

$$t'_e = \tau_1 + 2\tau ; \quad (29)$$

$$t''_e = \tau_1 + \tau + \Gamma_1 m_1 \tau; \quad (30)$$

$$t'''_e = \tau_1 + \tau + \Gamma_2 m_2 \tau; \quad (31)$$

where the first response yields the undisturbed information about the first color (transition I–II), while the second response has the transformed temporal structure of the second color (transition I–III), moreover, the real–time scale of this response is transformed by applying the factor $1/\Gamma_1 m_1$. The temporal scale of the third response is similarly transformed (by applying the factor $1/\Gamma_2 m_2$). The echo–hologram responses on the transitions I–III and I–IV have similar structures. Figure 10 shows virtual echo–hologram responses. Here A_i and B_i are the events, information about which was embedded in the object pulse.

When the first pulse is the object one, reverse sequence of events recorded in the echo–hologram will be observed simultaneously with transformation of the time scale.

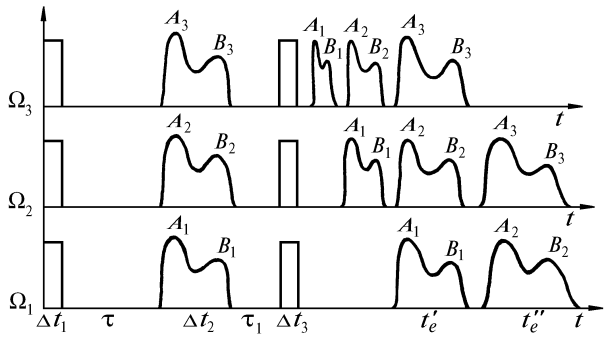

FIG. 10. Virtual stimulated color echo–hologram responses.

When the inhomogeneous broadening of lines on different transitions are uncorrelated, the echo–hologram response will contain only the responses at the moment t'_e, without any transformation of the real–time scale.

One may choose a $LaF_3:Pr^{3+}$ crystal for a resonance medium to record and transform color echo–holograms. Detailed experiments to study the salient features of formation of photon echo–signals have already been carried out on the $^3H_4 - ^3P_0$ (see Refs. 36–37) and $^3H_4 - ^1D_2$ (see Ref. 38) transitions in that crystal. Note also that the echo–hologram may be reproduced using the state $^3H_4$ as well as other energy transitions, e.g., $^3H_4 - ^3P_{1,2}$. In such cases the color of the object may be changed together with the real–time scale and the waveform of the response field. Taking into account that the number of the alternative methods of three–pulse excitation of signals of the stimulated photon echo in multilevel systems is large, such transformations may be performed in various regimes including the multi–quanta regime.

The present study was supported by the Russian Fund for Fundamental Studies.

REFERENCES

1. Yu.N. Denisjuk, J. Appl. Spectrosc. **33**, No. 3, 397–414 (1980).
2. D.I. Stasel'ko, in: Tr. Gos. Opt. Inst. **67**, No. 201, 12–36 (1988).
3. H. Gerretsen, Appl. Phys. Lett. **10**, No. 9, 239–241 (1967).
4. H. Boersch and H. Eichler, Z. Angew. Phys. **22**, No. 5, 378–379 (1967).
5 E.I. Shtyrkov, Pis'ma Zh. Eksp. Tekh. Fiz. **12**, No. 3, 134–137 (1970).
6. Yu.I. Ostrovskii, et al., Pis'ma Zh. Eksp. Tekh. Fiz. **1**, No. 22, 1030–1033 (1975).
7. S. Griffen and C.V. Heer, Appl. Phys. Lett. **33**, No. 10, 865–866 (1978).
8. A.K.Rebane, R.K. Kaarli, and P.M. Saari, Pis'ma Zh. Eksp. Tekh. Fiz. **38**, No. 7, 320–323 (1983).
9. V.G. Bespalov and D.I. Staselko, Pis'ma Zh. Eksp. Tekh. Fiz. **40**, No. 22, 1364–1369 (1984).
10. D. Phillion, Appl. Phys. Lett. **27**, No. 2, 85–87 (1975).
11. E.I. Shtyrkov and V.V. Samartsev, in: *Electromagnetic Hyperradiation* (Kazan' Phys. Inst. of the Academy of Sciences of the USSR, Kazan', 1975), pp. 398–426.
12. E.I. Shtyrkov and V.V. Samartsev, Opt. Spectrosk. **40**, No. 2, 392 (1976).
13. V.V. Samartsev and E.I. Shtyrkov, Fiz. Tverd. Tela **18**, No. 10, 3140–3141 (1976).
14. V.V. Samartsev and E.I. Shtyrkov, in: *Spectroscopy of Crystals* (Nauka, Leningrad, 1978), pp. 108–116.
15. V.V. Samartsev and E.I. Shtyrkov, in: *Fundamentals of Optical Memory and Media* (Vysshaya Shkola, Kiev, 1978), No. 9, pp. 100–109.
16. U.Kh. Kopvillem and V.R. Nagibarov, in: *Abstracts of Reports at the Ninth All–Union Conf. Low–Temp. Phys.* (Leningrad State Univ. Publ. House, Leningrad, 1962), p. 28.
17. U.Kh. Kopvillem and V.R. Nagibarov, Fiz. Met. and Metallov **15**, No. 2, 313–315 (1963).
18. A. Rebane, R. Kaarli, and P. Saari, Izvest. Akad. Nauk Estonsk. SSR, Fiz. Mat. **34**, No. 3, 328–330 (1985).
19. A. Rebane, R. Kaarli, P. Saari, et al., Opt. Commun. **47**, No. 3, 173–176 (1983).
20. L.A. Nefed'ev, Opt. Spectrosk. **56**, No. 5, 889–892 (1984).
21. L.A. Nefed'ev, Opt. Spectrosk. **58**, No. 4, 854–859 (1985).

22. L.A. Nefed'ev, Opt. Spectrosk. **56**, No. 5, 961–963 (1984).
23. V.A. Zuikov, L.A. Nefed'ev, and V.V. Samartsev, Opt. Spectrosk. **57**, No. 5, 929–931 (1984).
24. L.A. Nefed'ev, Opt. Spectrosk. **59**, No. 4, 841–846 (1985).
25. L.A. Nefedjev, Zh. Prikl. Spectrosk. **44**, No. 4, 664–669 (1986).
26. L.A. Nefed'ev, Opt. Spectrosk. **61**, No. 2, 387–394 (1986).
27. L.A. Nefedjev, Izv. Akad. Nauk SSSR, Fiz. **50**, No. 8, 1551–1558 (1986).
28. L.A. Nefedjev and V.V. Samartsev, Phys. Status Solidi **88a**, 631–635 (1985).
29. S.M. Zakharov and É.A. Manykin, Zh. Eksp. Tekh. Fiz. **91**, No. 4, 1289–1301 (1976).
30. L.A. Nefedjev and V.V. Samartsev, Opt. Spectrosk. **62**, No. 3, 701–703 (1987).
31. L.A. Nefedjev and V.V. Samartsev, Zh. Prikl. Spectrosk. **47**, No. 4, 638–703 (1987).
32. H. Jenkins and J. Watts, *Spectral Analysis and its Applications* [Russian translation] (Mir, Moscow, 1971), 316 pp.
33. T.W. Mossbery, Opt. Lett. **7**, No. 2, 77–79 (1982).
34. V.A. Zuikov, L.A. Nefed'ev, and V.V. Samartsev, in: *Applied Problems of Holography* (Leningrad Inst. Nucl. Phys. Press., Leningrad, 1982), pp. 175–179.
35. V.A. Zuikov, V.V. Samartsev, and R.G. Usmanov, Pis'ma Zh. Eksp. Tekh. Fiz. **32**, No. 4, 293–297 (1980).
36. Y.C. Chen, K. Chiang, and S.R. Hartmann, Opt. Commun. **29**, No. 2, 181–185 (1979).
37. I.B.W. Morsink and D.A. Wiersma, Chem. Phys. Lett. **65**, No. 1, 105–108 (1979).
38. E.A. Whittaker and S.R. Hartmann, Phys. Rev. **B26**, No. 7, 3617–3621 (1982).